THE JOURNAL OF PHYSICAL CHEMISTRY B LETTERS

2006, *110,* 14525−14528
Published on Web 05/19/2006

Noncontact Dielectric Friction

Seppe Kuehn, John A. Marohn, and Roger F. Loring*

Department of Chemistry and Chemical Biology, Baker Laboratory, Cornell University, Ithaca, New York 14853

Received: March 25, 2006; In Final Form: April 26, 2006

Dielectric fluctuations are shown to be the dominant source of noncontact friction in high-sensitivity scanning probe microscopy of dielectric materials. Recent measurements have directly determined the friction acting on custom-fabricated single-crystal silicon cantilevers whose capacitively charged tips are located 3−200 nm above thin films of poly(methyl methacrylate), poly(vinyl acetate), and polystyrene. Differences in measured friction among these polymers are explained here by relating electric field fluctuations at the cantilever tip to dielectric relaxation of the polymer.

An ion moving in a polar fluid experiences a drag, termed dielectric friction, resulting from fluctuating electrostatic forces exerted on the ion by molecules in the liquid.[1−4] Here, we demonstrate that a similar mechanism can be responsible for the noncontact friction[5,6] experienced by the probe in high-sensitivity scanning probe microscopy[7] of dielectrics. Such noncontact friction plays a central role in a variety of phenomena including micro- and nanomechanics[8] and can set the limits on sensitivity in scanning probe microscopies,[7,9] including magnetic resonance force microscopy.[10−12]

A previous report[13] has described the first use of a high-sensitivity single-crystal silicon cantilever to probe noncontact friction at distances of 3−200 nm above polymer thin films. The cantilever used in this study, shown schematically in Figure 1, has dimensions of 250 μm × 5 μm × 340 nm, resulting in a force constant of $k = 7 \times 10^{-4}$ N/m and a fundamental frequency of $\omega_c/2\pi = 7.385$ kHz. The platinum-coated cantilever tip has a radius of approximately 30 nm. The cantilever oscillates parallel to the sample surface in the direction labeled x in Figure 1, in contrast to the configuration of conventional atomic force microscopy. The sample is a polymer film of thickness 12 nm $\leq h \leq$ 450 nm, spin-cast onto an epitaxial Au(111) substrate. The tip−sample voltage, V_{ts} in Figure 1, is applied to the substrate, while the cantilever is grounded. This applied voltage produces a charge $q = C(V_{ts} - \phi)$ on the cantilever tip, with C the tip−sample capacitance and ϕ the contact potential difference between the tip and the substrate.

The total friction Γ_t is determined[7,13] from the time constant τ of a cantilever ringdown; $\Gamma_t = 2k/\omega_c^2\tau$. The total friction $\Gamma_t = \Gamma_0 + \Gamma_s$ is composed of an intrinsic friction Γ_0 and a noncontact friction generated by tip−sample interactions, Γ_s. In high vacuum and at room temperature, measurements with the tip far from the sample surface yield $\Gamma_0 = 6 \times 10^{-13}$ N s/m. Measured values of Γ_s are obtained by subtracting this constant Γ_0 from Γ_t. Measurements of Γ_t for poly(methyl methacrylate) (PMMA, $M_w = 145\,000$, $M_w/M_n \leq 1.05$), poly(vinyl acetate) (PVAc, $M_w = 147\,000$, $M_w/M_n \leq 3.1$), and polystyrene (PS, $M_w = 143\,000$, $M_w/M_n \leq 1.09$) for a variety of film thicknesses h and tip−sample separations d are reported in ref 13, where it is shown that these polymers of similar dielectric constant[13] ($\epsilon_{PMMA} = 3.9$; $\epsilon_{PVAc} = 3.4$; $\epsilon_{PS} = 2.5$)

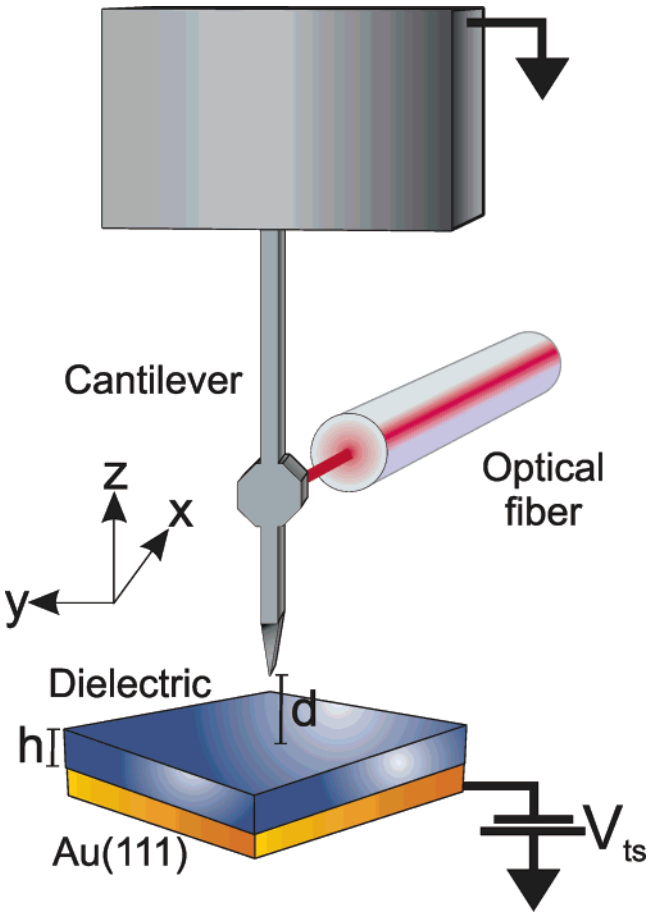

Figure 1. Schematic version of the measurement is shown, with d the tip−sample separation and h the film thickness. The cantilever oscillates along the x direction, parallel to the surface. The tip−sample voltage V_{ts} is applied to the gold layer under the polymer film, while the cantilever is grounded.

10.1021/jp061865n CCC: $33.50

produce significantly different noncontact friction. These studies further demonstrate that the measurement is sensitive to subsurface dynamics and that the friction is not dominated by surface adsorbates, such as water.[13]

The purpose of this letter is to present a relation between the noncontact friction Γ_s and the complex-valued dielectric response of the sample $\hat{\epsilon}(\omega)$, and to show that this analysis is consistent with the measurements. The charged cantilever tip interacting with a dielectric surface has been demonstrated in the laboratory in two ways to act as a harmonic oscillator driven by a fluctuating force $q\delta E_x(t)$, with $\delta E_x(t)$ the fluctuating electric field at the cantilever tip in the direction of motion. First, $\langle x^2\rangle$, the mean-squared variation in the cantilever displacement, is independent of the magnitude of the friction, in agreement with the prediction of the equipartition theorem, $\langle x^2\rangle = k_B T/k$. Second, Γ_s is always found to be quadratic in the applied voltage V_{ts} and, by implication, in the tip charge q. In this regime of linear response, the sample-induced contribution to the total friction obeys the fluctuation−dissipation[7,14] relation

$$\Gamma_s = \frac{q^2}{k_B T}\int_0^\infty \mathrm{d}t\, \cos(\omega_c t) C_E(t) \tag{1}$$

$$C_E(t) \equiv \langle \delta E_x(t)\delta E_x(0)\rangle \tag{2}$$

The angular brackets in eq 2 represent an equilibrium average for $q = 0$. We compute Γ_s by connecting the cosine transform of $C_E(t)$ in eq 1 to $\hat{\epsilon}(\omega)$, which may be measured independently.

We begin by determining a relation between the static dielectric constant of the polymer $\epsilon \equiv \hat{\epsilon}(0)$ and the mean-squared electric field fluctuation at the cantilever tip, $C_E(0) = \langle(\delta E_x)^2\rangle$. We consider a fictitious dipole moment of magnitude μ oriented along x at the location of the cantilever tip. A dipole is chosen for this analysis because its energy is linear in the electric field produced by the sample. This dipole will polarize the sample, generating a reaction field[15] at the location of the dipole. The average value of this fluctuating reaction field is denoted E_x. In the regime of linear response, E_x is linear in the dipole moment and proportional to the mean-squared field fluctuation generated by the sample at the location of the cantilever tip in the absence of the fictitious dipole

$$\langle(\delta E_x)^2\rangle = \frac{k_B T}{\mu} E_x \tag{3}$$

The reaction field E_x may be determined from macroscopic electrostatics by solving the boundary-value problem[16] appropriate to a dipole oriented parallel to, and located a distance d above, a dielectric slab of thickness h backed by a conductor. Application of the method of images yields

$$E_x = \mu\zeta\left\{\frac{1}{8d^3} - \frac{\zeta}{8(h+d)^3} - (1-\zeta^2)\sum_{j=0}^{\infty}(-\zeta)^j\left[\frac{1}{2d+(4+2j)h}\right]^3\right\} \tag{4}$$

$$\zeta \equiv \frac{\epsilon - 1}{\epsilon + 1} \tag{5}$$

The first term in eq 4 is the reaction field in the limit of an infinitely thick dielectric slab, with ζ a dielectric screening function arising in planar geometries, and the infinite series gives corrections for finite slab thickness h. For a thin dielectric sample, it is convenient to sum the series in eq 4 by applying the identity $b^{-3} = (1/2)\int_0^\infty \mathrm{d}y y^2 \exp(-by)$ to each term in the series to yield

$$E_x = \frac{\mu\zeta}{2d^3}\int_0^\infty \mathrm{d}x\, x^2\, \mathrm{e}^{-2x}\left[\frac{(1-\mathrm{e}^{-4(h/d)x})}{1+\zeta\,\mathrm{e}^{-2(h/d)x}}\right] \tag{6}$$

The mean-squared electric field fluctuation at the cantilever tip is then given by eq 3 with the expression for the reaction field in eq 4 or 6. This relationship, correct within linear response theory for a homogeneous, continuum dielectric, can be approximately generalized to the time domain, as is required to evaluate the friction in eq 1.

To extend the static result in eq 6 to the time domain, we consider the time-dependent reaction field generated by a dielectric medium polarized by a time-dependent external dipole introduced at $t = 0$. The Fourier−Laplace transform of the resulting reaction field $\hat{E}_x(\omega) \equiv \int_0^\infty \mathrm{d}t \exp(-i\omega t)E_x(t)$ is given in classical-mechanical linear response theory by

$$\hat{E}_x(\omega) = -\frac{\hat{\mu}(\omega)}{k_B T}[i\omega\hat{C}_E(\omega) - C_E(0)] \tag{7}$$

with $\hat{\mu}(\omega)$ the Fourier−Laplace transform of the time-dependent dipole moment and $\hat{C}_E(\omega)$ the transform of $C_E(t)$. We next invoke a quasi-static approximation that has been successfully applied to time-dependent solvation phenomena in molecular fluids, such as the dynamic Stokes shift of a solvatochromic dye,[17−20] in which $\hat{E}_x(\omega)$ is determined by solving a macroscopic electrostatic boundary-value problem for a dielectric with complex dielectric function $\hat{\epsilon}(\omega)$. In this approximation, the Maxwell equation $\epsilon\nabla\cdot\mathbf{E} = 4\pi\rho$ for static electric field $\mathbf{E}$ and charge distribution ρ is assumed to hold at finite frequency, $\hat{\epsilon}(\omega)\nabla\cdot\hat{\mathbf{E}}(\omega) = 4\pi\hat{\rho}(\omega)$. For the case in which a charge distribution $\rho(t)$ is switched on at $t = 0$ and attains an asymptotic limiting value of ρ as $t \to \infty$, the approximate frequency-dependent Maxwell equation approaches the correct limit as $\omega \to 0$: $\hat{\mathbf{E}}(\omega) \to \mathbf{E}/i\omega$, $\hat{\rho}(\omega) \to \rho/i\omega$, and $\hat{\epsilon}(\omega) \to \epsilon$. Application of this result at nonzero frequency represents an adiabatic approximation.[17] Within this approximation, the result in eq 6 can be generalized by replacing the dipole moment, electric field, and dielectric function at zero frequency with their complex-valued counterparts at finite frequency

$$\hat{E}_x(\omega) = \frac{\hat{\mu}(\omega)\hat{\zeta}(\omega)}{2d^3}\int_0^\infty \mathrm{d}x\, x^2\, \mathrm{e}^{-2x}\left[\frac{(1-\mathrm{e}^{-4(h/d)x})}{1+\hat{\zeta}(\omega)\mathrm{e}^{-2(h/d)x}}\right] \tag{8}$$

The dielectric function enters this expression through the frequency-dependent generalization of eq 5: $\hat{\zeta}(\omega) = (\hat{\epsilon}(\omega) - 1)/(\hat{\epsilon}(\omega) + 1)$. Substituting this relation for $\hat{E}_x(\omega)$ into eq 7 permits the connection of the correlation function $\hat{C}_E(\omega)$ to $\hat{\epsilon}(\omega)$. The cosine transform in eq 1 is the real part of $\hat{C}_E(\omega)$, so that the sample-induced friction affecting the cantilever tip is

$$\Gamma_s = \frac{q^2\hat{\zeta}''(\omega_c)}{2\omega_c d^3} \times \int_0^\infty \mathrm{d}x\, x^2\, \mathrm{e}^{-2x}\frac{1-\mathrm{e}^{-4(h/d)x}}{[1+\hat{\zeta}'(\omega_c)\mathrm{e}^{-2(h/d)x}]^2 + [\hat{\zeta}''(\omega_c)]^2\mathrm{e}^{-4(h/d)x}} \tag{9}$$

with the real and imaginary parts of $\hat{\zeta}(\omega)$ defined by $\hat{\zeta}(\omega) = \hat{\zeta}'(\omega) + i\hat{\zeta}''(\omega)$.

According to eq 9, the noncontact friction is determined by the complex dielectric function evaluated at the resonance

frequency of the cantilever, which is $\omega_c/2\pi = 7.385$ kHz for these measurements. The experiments of ref 13 thus complement previous studies by Israeloff and co-workers[21−23] who used scanning probe microscopy to measure dielectric fluctuations in glassy polymer samples at frequencies of ≤1 Hz. The noncontact friction in eq 9 was calculated for a charged cantilever tip, and hence vanishes at $q = 0$. Zurita-Sanchez et al.[6] have computed the noncontact friction of an uncharged and polarizable probe, produced by fluctuating electromagnetic forces from a sample. A qualitative conclusion of their analysis is that the noncontact friction produced by a metal layer over a dielectric substrate is dominated by the dielectric.[6] This prediction is not supported by the measurements reported in ref 13, suggesting that this analysis of the friction on an uncharged probe does not describe the case of a charged probe discussed here.

Determining the magnitude of Γ_s from eq 9 requires calculation of the charge q on the cantilever tip, which in turn necessitates modeling the tip−sample capacitance C through the introduction of additional approximations.[13] The capacitance C depends on the geometry of the tip−sample system and on the static dielectric constant of the polymer film.[24] Calculations of Γ_s and its dependence on d and h based on an assumed spherical geometry for the cantilever tip are presented in ref 13 and are shown to agree qualitatively with measurements. Here, we make the simplifying assumption that for fixed[13] d and $V_{ts} - \phi$, C is approximately constant for different polymer samples, so that q in eq 9 is independent of polymer species at fixed d. In this case, we can avoid the model-dependent calculation of C by forming the ratio of Γ_s values for two different polymers at constant tip−sample separation d. According to eq 9, the charge cancels out of this ratio, and the friction ratio depends only on h/d and the dielectric functions of the two materials, and contains no adjustable parameters. Evaluation of the friction ratio from eq 9 requires measurement of the absorptive and dispersive parts of the dielectric response of the polymer sample at $\omega = \omega_c$, the resonance frequency of the cantilever. We measured[13] dielectric spectra of 450-nm-thick films of PMMA and PVAc, which do not differ significantly from bulk values at $\omega_c/2\pi \approx 7$ kHz and used literature values for the dielectric function of bulk PS.[25] Dielectric relaxation in films of these three polymers[26,27] has been shown to depend significantly on film thickness for $h \leq 100$ nm, but such effects are generally small for thicknesses on the order of 450 nm. Glass transition temperatures for high molecular weight bulk samples of these polymers[26,27] are $T_g^{PVAc} \approx 303$ K, $T_g^{PMMA} \approx 373$ K, and $T_g^{PS} \approx 373$ K. Reductions[28] from these bulk values[26,27] for a film thickness of 450 nm are expected to be small, so that all films may be taken to be glassy at room temperature.

The three friction ratios for each pair of polymer samples are plotted in Figure 2 for 8 nm ≤ d ≤ 20 nm and fixed film thickness $h = 450$ nm. Measured ratios are shown by symbols, connected by line segments to guide the eye. The green circles show $\Gamma_s^{PMMA}/\Gamma_s^{PS}$, the red squares show $\Gamma_s^{PVAc}/\Gamma_s^{PS}$, and the blue triangles show $\Gamma_s^{PMMA}/\Gamma_s^{PVAc}$. Over this range of d and for a relatively thick film, these ratios do not depend significantly on d, and hence, we interpret the variation displayed in Figure 2 as noise that provides an estimate for error bars on the mean values of these ratios. The resulting mean values of these friction ratios are $\Gamma_s^{PMMA}/\Gamma_s^{PS} = 75 \pm 21$, $\Gamma_s^{PVAc}/\Gamma_s^{PS} = 18 \pm 5$, and $\Gamma_s^{PMMA}/\Gamma_s^{PVAc} = 4.4 \pm 0.4$. The prediction of eq 9 for each ratio is shown by the continuous curves in Figure 2, with the same color scheme as for the data. The calculated friction ratios do not vary significantly with d for $h \gg d$. Dashed lines show error bars for the calculated friction ratios, which arise from uncertainties in the measured dielectric functions. The calculated friction ratios are $\Gamma_s^{PMMA}/\Gamma_s^{PS} = 71 \pm 7$, $\Gamma_s^{PVAc}/\Gamma_s^{PS} = 27 \pm 3$, and $\Gamma_s^{PMMA}/\Gamma_s^{PVAc} = 2.6 \pm 0.3$, within 50% of the measured results. Friction measurements for PMMA and PVAc could be carried out for larger d than for PS, and the ratio $\Gamma_s^{PMMA}/\Gamma_s^{PVAc}$ is shown up to $d = 60$ nm in Figure 3, in which the ordinate shows a linear scale in contrast to Figure 2. The greater range of d in Figure 3 reveals that the ratio $\Gamma_s^{PMMA}/\Gamma_s^{PVAc}$ increases with increasing d in a way that is not reproduced by the calculation, although the signal-to-noise ratio is also seen to decrease with increasing d. One possible explanation for this discrepancy between prediction and measurement lies with the assumption described in the preceding paragraph that the charge q may be taken to be independent of polymer sample for fixed d and voltage. Deviations from this scenario could result in additional d dependence for the measured friction ratio that would not be captured by the calculation. Also, the present analysis treats the polymer film as dynamically homogeneous, so that any variation in polymer dynamics with depth in the

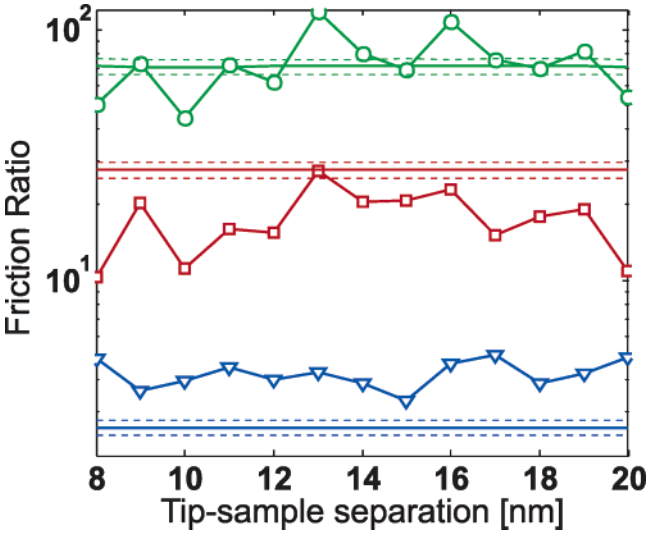

Figure 2. The ratio of friction coefficients for pairs of polymers is shown for 8 nm ≤ d ≤ 20 nm at fixed film thickness $h = 450$ nm. Symbols show the measured friction ratios $\Gamma_s^{PMMA}/\Gamma_s^{PS}$ (green circles), $\Gamma_s^{PVAc}/\Gamma_s^{PS}$ (red squares), and $\Gamma_s^{PMMA}/\Gamma_s^{PVAc}$ (blue triangles). The predictions of eq 9 together with dielectric relaxation measurements are shown by the solid curves using the same color assignment as the data. Dashed lines indicate the error bars on the calculated friction ratios, which are associated with the dielectric relaxation measurements.

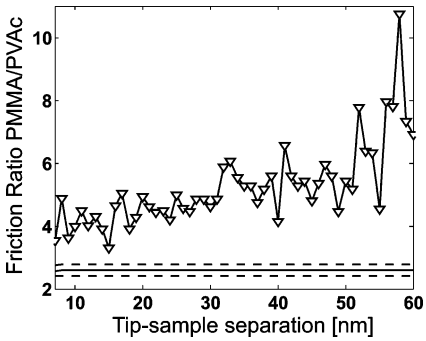

Figure 3. The ratio of friction coefficients $\Gamma_s^{PMMA}/\Gamma_s^{PVAc}$ is shown for 7 nm ≤ d ≤ 60 nm at fixed film thickness $h = 450$ nm, a larger range of tip−sample separation than covered in Figure 2. Note the linear scale of the ordinate, in contrast to Figure 2. As in Figure 2, the solid curve shows the prediction of eq 9, with error bars indicated by dashed lines.

film[29−32] that is dependent on molecular identity could result in additional d dependence in the friction ratio not included in eq 9. The calculation of the friction from eq 9, together with measured dielectric spectra, reproduces the trends shown by the measured friction, that $\Gamma_s^{PMMA} > \Gamma_s^{PVAc} > \Gamma_s^{PS}$.

The comparison of calculation and measurement in Figure 2 is performed without any adjustable parameters. This agreement between the continuum dielectric calculation and experiment strongly supports the picture that the noncontact friction in these room-temperature experiments is dominated by thermal dielectric fluctuations in the polymer films. In addition to elucidating a source of noncontact friction over organic materials, this analysis suggests that this measurement promises future applications as a local probe of dielectric fluctuations[21−23] in thin films. It remains for future studies to compare the dependence on temperature and frequency of the noncontact friction over dielectrics to the predictions of eq 9.

Acknowledgment. R.F.L. acknowledges support from the National Science Foundation through grants no. CHE0105623 and no. CHE0413992, and from the Petroleum Research Fund of the American Chemical Society. S.K. and J.A.M. acknowledge support from the National Institutes of Health (5R01GM-070012), the ARO/NSA/ARDA Quantum Computing Program (DAAD19-02-1-0064), Cornell University, and the Army Research Office Multiuniversity Research Initiative (W911NF-05-1-0403). S.K. acknowledges additional support from the Society of Analytical Chemists of Pittsburgh through the Analytical Division of the American Chemical Society.

References and Notes

(1) Wolynes, P. G. *Annu. Rev. Phys. Chem.* **1980**, *31*, 345.
(2) Felderhof, B. U. *Mol. Phys.* **1983**, *45*, 1003.
(3) Stiles, P. J.; Hubbard, J. D. *Chem. Phys. Lett.* **1984**, *105*, 655.
(4) Hynes, J. T. *Annu. Rev. Phys. Chem.* **1985**, *36*, 573.
(5) Persson, B. N. J.; Zhang, Z. *Phys. Rev. B* **1998**, *57*, 7327.
(6) Zurita-Sanchez, J. R.; Greffet, J. J.; Novotny, L. *Phys. Rev. A* **2004**, *69*, 022902.
(7) Stipe, B. C.; Mamin, H. J.; Stowe, T. D.; Kenny, T. W.; Rugar, D. *Phys. Rev. Lett.* **2001**, *87*, 96801.
(8) Volokitin, A. I.; Persson, B. N. J. *Phys. Rev. Lett* **2003**, *91*, 106101.
(9) Jenkins, N. E.; DeFlores, L. P.; Allen, J.; Ng, T. N.; Garner, S. R.; Kuehn, S.; Dawlaty, J. M.; Marohn, J. A. *J. Vac. Sci. Technol., B* **2004**, *22*, 909.
(10) Garner, S. R.; Kuehn, S.; Dawlaty, J. M.; Jenkins, N. E.; Marohn, J. A. *Appl. Phys. Lett.* **2004**, *84*, 5091.
(11) Rugar, D.; Budakian, R.; Mamin, H. J.; Chui, B. W. *Nature (London)* **2004**, *430*, 329.
(12) Mamin, H. J.; Budakian, R.; Chui, B. W.; Rugar, D. *Phys. Rev. B* **2005**, *72*, 024413.
(13) Kuehn, S.; Loring, R. F.; Marohn, J. A. *Phys. Rev. Lett.* **2006**, *96*, 156103.
(14) Zwanzig, R. *J. Stat. Phys.* **1973**, *9*, 215.
(15) Onsager, L. *J. Am. Chem. Soc.* **1936**, *58*, 1486.
(16) Lyukyotsov, S. F.; Paramonov, P. B.; Sharipov, R. A.; Sigalov, G. *Phys. Rev. B* **2004**, *70*, 174110.
(17) Bagchi, B.; Oxtoby, D. W.; Fleming, G. R. *Chem. Phys.* **1984**, *86*, 257.
(18) Wolynes, P. G. *J. Chem. Phys.* **1987**, *86*, 5133.
(19) Rips, I.; Klafter, J.; Jortner, J. *J. Chem. Phys.* **1988**, *88*, 3246.
(20) Zhou, H.-X.; Bagchi, B.; Papazyan, A.; Maroncelli, M. *J. Chem. Phys.* **1992**, *97*, 9311.
(21) Russell, E. V.; Israeloff, N. E.; Walther, L. E.; Gomariz, H. A. *Phys. Rev. Lett*. **1998**, *81*, 1461.
(22) Russell, E. V.; Israeloff, N. E. *Nature (London)* **2000**, *408*, 695.
(23) Sinnathamby, K. S.; Oukris, H.; Israeloff, N. E. *Phys. Rev. Lett.* **2005**, *95*, 067205.
(24) Cherniavskaya, O.; Chen, L.; Weng, V.; Yuditsky, L.; Brus, L. E. *J. Phys. Chem. B* **2003**, *107*, 1525.
(25) Brandrup, J.; Immergut, E. *Polymer Handbook*; Wiley: New York, 1965.
(26) Fukao, K.; Miyamoto, Y. *Phys. Rev. E* **2000**, *61*, 1743.
(27) Fukao, K.; Uno, S.; Miyamoto, Y.; Hoshino, A.; Miyaji, H. *Phys. Rev. E* **2001**, *64*, 051807.
(28) Keddie, J. L.; Jones, R. A. L.; Cory, R. A. *Europhys. Lett*. **1994**, *27*, 59.
(29) Priestly, R. D.; Ellison, C. J.; Broadbelt, L. J.; Torkelson, J. M. *Science* **2005**, *309*, 456.
(30) Zhu, X.; Farrar, R. A.; Fourkas, J. T. *J. Phys. Chem. B* **2005**, *109*, 12724.
(31) Wang, L.-M.; He, F.; Richert, R. *Phys. Rev. Lett*. **2004**, *92*, 095701.
(32) He, F.; Wang, L.-M.; Richert, R. *Phys. Rev. B* **2005**, *71*, 144205.